

Quantification of aneurysm wall enhancement in intracranial fusiform aneurysms and related predictors based on high-resolution magnetic resonance imaging: a validation study

Fei Peng*, Mingzhu Fu*, Jiexiang Xia*, Hao Niu, Lang Liu, Xin Feng, Peng Xu, Xiaoyan Bai, Zhiye Li, Jigang Chen, Xin Tong, Xiaoxin He, Boya Xu, Xuge Chen, Hongyi Liu, Binbin Sui, Yonghong Duan, Rui Li* and Aihua Liu* 

Abstract

Background: Aneurysm wall enhancement (AWE) in high-resolution magnetic resonance imaging (HR-MRI) has emerged as a new imaging biomarker of intracranial aneurysm instability.

Objective: To determine a standard method of AWE quantification for predicting fusiform intracranial aneurysms (FIAs) stability by comparing the sensitivity of each parameter in identifying symptomatic FIAs. The predictors of AWE and FIA types were also identified.

Methods: We retrospectively analyzed consecutive fusiform aneurysm patients who underwent HR-MRI from two centers. The aneurysm-to-pituitary stalk contrast ratio (CR_{stalk}), aneurysm enhancement ratio, and aneurysm enhancement index were extracted, and their sensitivities in discriminating aneurysm symptoms were compared using the receiver-operating characteristic curve. Morphological parameters of fusiform aneurysm were extracted based on 3D vessel model. Uni- and multivariate analyses of related predictors for AWE, CR_{stalk} , and FIA types were performed, respectively.

Results: Overall, 117 patients (mean age, 53.3 ± 11.7 years; male, 75.2%) with 117 FIAs underwent HR-MRI were included. CR_{stalk} with the maximum signal intensity ($CR_{\text{stalk-max}}$) had the highest sensitivity in identifying symptomatic FIAs with an area under the curve value (0.697) and a cut-off value of 0.90. The independent predictors of AWE were aneurysm symptoms [(odds ratio) $OR = 3.754$, $p = 0.003$], aspirin use ($OR = 0.248$, $p = 0.037$), and the maximum diameter of the cross-section ($OR = 1.171$, $p = 0.043$). The independent predictors of $CR_{\text{stalk-max}}$ were aneurysm symptoms ($OR = 1.289$, $p = 0.003$) and posterior circulation aneurysm ($OR = 1.314$, $p = 0.001$). Transitional-type showed higher rates of hypertension and mural thrombus over both dolichoectatic- and fusiform-type FIAs.

Conclusion: $CR_{\text{stalk-max}}$ may be the most reliable parameter to quantify AWE to distinguish symptomatic FIAs. It also has the potential to identify unstable FIAs. Several factors contribute to the complex pathophysiology of FIAs and need further validation in a larger cohort.

Keywords: fusiform aneurysm, magnetic resonance imaging, symptoms, validation, vessel wall imaging

Received: 22 February 2022; revised manuscript accepted: 18 May 2022.

Ther Adv Neurol Disord

2022, Vol. 15: 1–14

DOI: 10.1177/
17562864221105342

© The Author(s), 2022.
Article reuse guidelines:
[sagepub.com/journals-](https://sagepub.com/journals-permissions)
permissions

Correspondence to:

Rui Li
Center for Biomedical
Imaging Research,
Department of Biomedical
Engineering, Tsinghua
University, Beijing, China.
leerui@tsinghua.edu.cn

Aihua Liu
Department of
Interventional
Neuroradiology, Beijing
Tiantan Hospital, Capital
Medical University, No.
119, South 4th Ring West
Road, Fengtai District,
Beijing 100070, China
Beijing Neurosurgical
Institute, Capital Medical
University, Beijing, China
China National Clinical
Research Center for
Neurological Diseases,
Beijing, China.
liuahua@doctor@163.com

Fei Peng
Jiexiang Xia
Hao Niu
Jigang Chen
Xin Tong
Xiaoxin He
Boya Xu
Xuge Chen
Hongyi Liu
Beijing Neurosurgical
Institute, Capital Medical
University, Beijing, China
Department of
Interventional
Neuroradiology, Beijing
Tiantan Hospital, Capital
Medical University, Beijing,
China

Mingzhu Fu
Center for Biomedical
Imaging Research,
Department of Biomedical
Engineering, Tsinghua
University, Beijing, China

Lang Liu
Department of
Neurosurgery, The
Third Xiangya Hospital,
Central South University,
Changsha, China

Xin Feng

Neurosurgery
Center, Department
of Cerebrovascular
Surgery, Engineering
Technology Research
Center of Education
Ministry of China on
Diagnosis and Treatment
of Cerebrovascular
Disease, Zhujiang
Hospital, Southern Medical
University, Guangzhou,
China

Guangdong Provincial
Key Laboratory on Brain
Function Repair and
Regeneration, Guangzhou,
China

Peng Xu

Yonghong Duan
Department of
Neurosurgery, The
Second Affiliated Hospital,
Hengyang Medical School,
University of South China,
Hengyang, China

Xiaoyan Bai

Zhiye Li
Binbin Sui
Department of Radiology,
Beijing Tiantan Hospital,
Capital Medical University,
Beijing, China

Tiantan Neuroimaging
Center of Excellence,
China National Clinical
Research Center for
Neurological Diseases,
Beijing, China

*Fei Peng, Mingzhu
Fu, and Jiaxiang Xia
contributed equally to this
article.

†Rui Li and Aihua Liu
corresponding authors
contributed equally to this
work.

Introduction

Intracranial aneurysms (IAs) affect nearly 3–5% of the entire population.¹ IA rupture leads to aneurysmal subarachnoid hemorrhage, followed by high morbidity and mortality.¹ Generally, IAs are dichotomized into saccular IAs (SIAs) and fusiform IAs (FIAs) based on their morphology.^{2,3} SIAs account for the majority, while FIAs only account for 3–13% of IAs.^{3–6} Recent studies have revealed that the physiological processes differ between SIAs and FIAs.^{3,7} Hemodynamically, FIAs may be subjected to lower hemodynamic stress than SIAs.^{7,8} Pathologically, FIAs may demonstrate more extensive pathological processes because they are associated with greater aneurysm wall enhancement (AWE) and more involved areas of the culprit artery than SIAs.³ On the basis of their pathological features, non-saccular aneurysms can be divided into three types: fusiform, dolichoectatic, and transitional.⁹

Aneurysm growth and rupture are mediated by inflammatory processes in the aneurysm wall.¹⁰ Recently, AWE on high-resolution magnetic resonance imaging (HR-MRI), which correlates with aneurysm wall inflammation and vasa vasorum, has been identified as a useful surrogate biomarker of unstable IAs.^{11,12} Thus, a standard quantification of AWE may help to delineate the borderline cases and screen those patients who need early intervention. Several studies have standardized AWE quantification in SIAs.^{13–15} One study has reported that the aneurysm-to-pituitary stalk contrast ratio (CR_{stalk}) with a cut-off value of 0.60 tends to have a higher sensitivity in discriminating unstable aneurysms than other AWE parameters (e.g. aneurysm enhancement ratio, AER; aneurysm enhancement index, AEI).¹³ However, there is currently no standard definition for AWE quantification of FIAs. Considering certain aneurysm symptoms (e.g. sentinel headache and oculomotor nerve palsy) reportedly strongly indicate aneurysm instability,¹⁶ it is, therefore, reasonable to determine a standard method of AWE quantification for predicting FIA stability by comparing the sensitivity of each parameter in identifying symptomatic FIAs. To understand the underlying mechanisms of IA progression, the risk factors for AWE of SIAs, which may include aneurysm symptoms, anti-inflammatory drugs, and aneurysm morphology, have been widely studied.^{16–18} In contrast, the related predictors of AWE in FIAs have received less attention. In addition, based on the

fact that FIAs, characterized by different classifications,^{8,9} present a wide spectrum of pathophysiology,⁸ investigating the related predictors of AWE and FIA types may help to understand the disease processes of vasculopathy.

We aimed to identify a standard method to quantify the AWE of FIAs. To further understand the physiological mechanisms of FIAs, related predictors of AWE and FIA types were also investigated.

Methods

Patients' characteristics

Consecutive patients with FIAs who underwent HR-MRI were retrospectively recruited from August 2015 to September 2021 at Beijing Tiantan Hospital and Center for Biomedical Imaging Research of Tsinghua University. Patients who harbored dissecting aneurysms, dural arteriovenous fistulas, arteriovenous malformations, Moya Moya disease or other cerebrovascular diseases, incomplete medical records, or poor image quality for AWE analysis, or without post-gadolinium sequencing on HR-MRI were excluded. The baseline characteristics of the patients, including aneurysm symptoms, hypertension, hyperlipidemia, diabetes mellitus, smoking status, and aspirin use, were obtained from medical records or telephone follow-up. Aneurysm symptoms were defined as sentinel headache and oculomotor nerve palsy, which strongly indicate aneurysm instability.¹⁶ Smoking status was defined as never smoking, current smoking, and former smoking, as outlined in our previous study.¹⁹ Aspirin use was defined as a daily intake of ≥ 81 mg aspirin in the recent 6 months or longer.¹⁶

Aneurysm characteristics

The characteristics of FIAs included fusiform type, location, maximum diameter (D_{max}), and maximum length (L_{max}). Dissecting aneurysms were defined as string sign, double lumen, intimal flap, alternation of stenosis and dilatation, arterial occlusion, or semilunar hematoma with luminal narrowing.^{20–22} Considering the inherent differences between dissecting aneurysms and other types of aneurysms, the Mizutani classification, which includes dissecting aneurysms, was not used in this study.

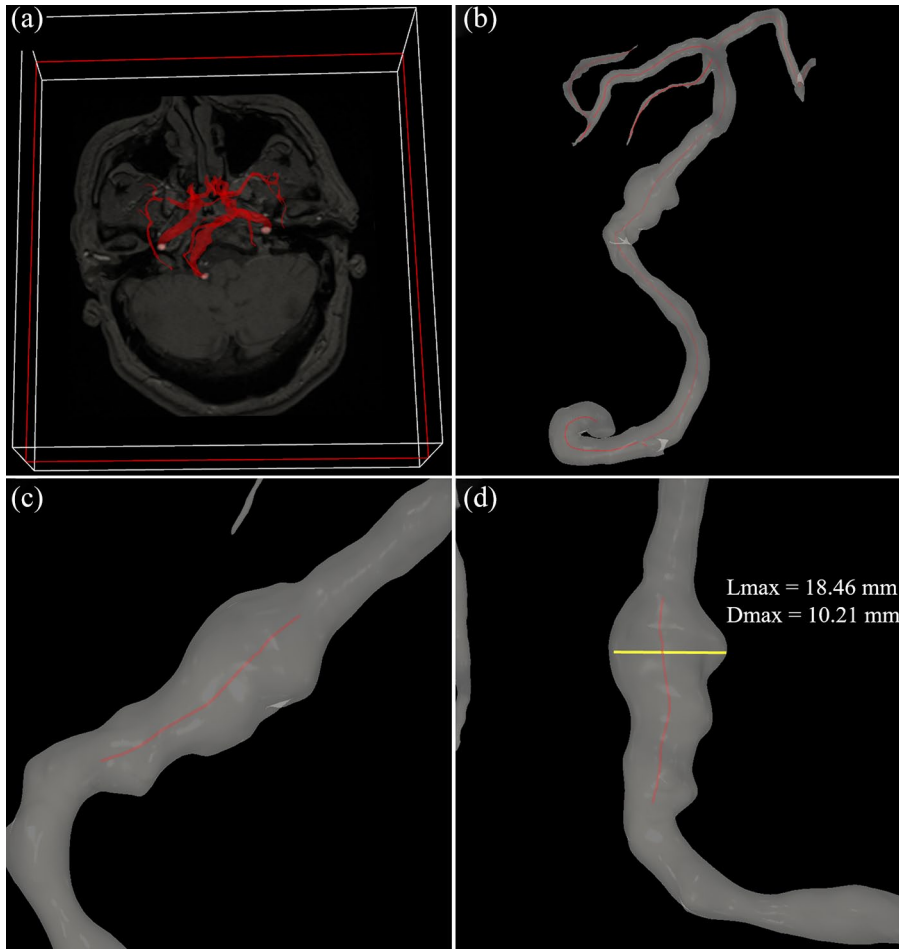


Figure 1. Quantification of D_{max} and L_{max} in the 3D space. (a) The 3D vessel model was first extracted from 3D TOF MRA. (b) The centerline of the vessel was then automatically extracted. (c and d) Finally, L_{max} was calculated based on the boundary definition, and D_{max} was measured in the cross-section.

One experienced reader with at least 20 years of neuroimaging diagnosis experience identified and excluded those dissecting aneurysms. Then, the included FIAs were classified based on Flemming's classification.^{8,9} Fusiform-type FIAs are characterized by dilatation of 1.5 times the diameter of the normal blood vessel, dolichoectatic-type FIAs are characterized by uniform dilatation of >1.5 times normal, while transitional-type FIAs are characterized by uniform dilatation of >1.5 times normal with overlapping dilatation of the part of the involved blood vessel.¹² The aneurysm location was divided into the anterior circulation and the posterior circulation.

D_{max} was defined as the greatest diameter in the cross-section,^{20,23,24} while L_{max} was defined as the length of the involved vessel with a boundary of

1.5 times the normal vessel.^{23,24} Three-dimensional (3D) time-of-flight (TOF) magnetic resonance angiography (MRA) was used to quantify D_{max} and L_{max} in the 3D space. Specifically, the 3D vessel model [Figure 1(a)] was first generated based on a workflow, including threshold segmentation, region growth, connected domain selection, and surface smoothing, using our in-house software programmed in Python. Second, to measure L_{max} , the centerline of the vessel was automatically extracted based on the feature tree growth algorithm [Figure 1(b)]. Next, the centerline of the FIA was isolated from the rest of the centerline network according to the boundary definition [Figure 1(c)]. Finally, L_{max} was calculated based on the isolated centerline, and D_{max} was measured in the cross-section [Figure 1(d)]. Mural thrombus was identified as a high signal in T1.²¹



Figure 2. Post-contrast 3D T1-weighted images revealed the 20mm² of corpus callosum (red circle), four points of the pituitary infundibulum (black plus), and fusiform aneurysm of the right vertebral artery (white triangle).

HR-MRI protocol

All MRI scans were performed using a 3.0-T MR scanner (Trio-Tim, Siemens Healthcare, Erlangen, Germany; Discovery 750, GE Healthcare, Milwaukee, WI, USA; Ingenia CX, Philips Healthcare, Best, the Netherlands) equipped with a 32-channel head coil. Three-dimensional TOF MRA was used to identify FIAs. High-resolution sequences included pre- and post-contrast 3D T1-weighted images (SPACE/CUBE/VISTA) with a voxel size of $0.7 \times 0.7 \times 0.7 \text{ mm}^3$. Six minutes after the injection of 0.1 mmol/kg gadopentetate dimeglumine (Gd, Magnevist; Bayer Schering Pharma AG), post-contrast T1-weighted imaging was performed.

AWE assessment

The AWE assessment was carried out using Horos (<https://horosproject.org/>). Two experienced readers with at least 5 years of neuroimaging diagnosis experience were blinded to patients' information to assess AWE. Any discrepancy was resolved by consensus with a third experienced reader. First, the pre- and post-contrast T1-weighted images of FIAs were manually co-registered in three planes (axial, coronal, and sagittal) using the same slide.¹⁶

Then, the region of interest of the aneurysm wall was extracted from the plane that covered the maximum aneurysm diameter. To avoid pseudo-enhancement of the aneurysm wall, pre- and post-contrast T1-weighted images were compared to define aneurysm wall thickness.¹⁶ SI_{wall} was defined as the signal intensity (SI) of the aneurysm wall on pre- or post-contrast T1-weighted images of FIAs at the plane covering the maximum aneurysm diameter in the cross-section and extending to the sites of 1.5 normal diameters of the parent vessel in both directions as the boundary (same boundary with the L_{max}).^{20,23,24} Meanwhile, the mean value of four randomized points in the pituitary stalk (SI_{stalk}) was calculated (Figure 2).¹³ $CR_{\text{stalk-average}}$ and $CR_{\text{stalk-max}}$ were calculated as the ratio of SI_{wall} over SI_{stalk} on post-contrast imaging, which used the mean and maximum SI, respectively.⁶ The AER was calculated as $(SI_{\text{wall-post}} - SI_{\text{wall-pre}}) / SI_{\text{wall-pre}}$.¹⁵ SI_{brain} was defined as the SI in the co-registered 20mm², which was drawn over the corpus callosum (Figure 2).¹⁵ Then, the AEI was calculated as $[(SI_{\text{wall-post}} / SI_{\text{brain-post}}) - (SI_{\text{wall-pre}} / SI_{\text{brain-pre}})] / (SI_{\text{wall-pre}} / SI_{\text{brain-pre}})$. Similarly, AER_{max} , AEI_{max} , AER_{average} , and AEI_{average} were calculated using the mean or maximum SI value.

Statistical analysis

All statistical analyses were conducted using SPSS version 22.0 (IBM Corp., Armonk, NY, USA). Continuous variables are expressed as mean \pm standard deviation, and categorical variables are expressed as frequency and percentage. A non-parametric test (Kruskal-Wallis H test) was used for statistical assessment of AWE parameters (CR_{stalk} , AER, and AEI) using the maximum and mean SI values, respectively. A p value of <0.05 was considered statistically significant. On the basis of aneurysm symptoms, which predict aneurysm instability, sentinel headache and oculomotor nerve palsy were used in the receiver-operating characteristic (ROC) curve analysis. Discrimination, which refers to the ability to discriminate symptomatic and asymptomatic FIAs, was assessed using the C-statistic [an area under the ROC curve (AUC) of 0.5 indicates no discriminative ability and an AUC of 1.0 indicates a perfect discriminative ability]. When the cut-off value of the AWE parameter with the highest sensitivity to discriminate aneurysm symptoms was defined, the AWE parameter was classified into two categories: non-AWE and AWE.

To identify the risk factors for AWE, the baseline characteristics of the patients and aneurysms were first examined in the univariate analysis (χ^2 test or Kruskal–Wallis H test). Variables with a p value of <0.20 were entered into the logistic regression analysis. To identify the risk factors of $CR_{\text{stalk-max}}$, those baseline characteristics were first examined in the general regression analysis. Variables with $p < 0.20$ were entered into the multiple linear regression analysis. To identify the risk factors for FIA type, those baseline characteristics were first examined in the univariate analysis (χ^2 test or Kruskal–Wallis H test). Variables with a p value of <0.10 were entered into the multinomial logistic regression analysis.

Results

Patient and aneurysm characteristics

A total of 117 patients (mean age, 53.3 ± 11.7 years; male, 75.2%) with FIAs were included in this study (Figure 3). Among them, 81 patients (69.2%) had fusiform-type FIAs, 21 patients (17.9%) had dolichoectatic-type FIAs, and 15 patients (12.8%) had transitional-type FIAs. The assessments of aneurysm morphology and AWE for these three types of FIA are summarized in Figure 4. Fifty patients (42.7%) presented with aneurysm symptoms, including 39 (33.3%) with sentinel headache and 11 (9.4%) with oculomotor nerve palsy. The characteristics of the patients and FIAs are listed in Table 1.

AWE quantification in discriminating symptomatic FIAs

The Kruskal–Wallis H test showed that patients with aneurysm symptoms had significantly higher $CR_{\text{stalk-max}}$ (0.99 versus 0.77, $p < 0.001$), AER_{max} (1.13 versus 0.68, $p = 0.037$), AEI_{max} (1.08 versus 0.84, $p = 0.022$), $CR_{\text{stalk-average}}$ (0.79 versus 0.65, $p = 0.001$), and AEI_{average} (0.80 versus 0.64, $p = 0.024$) values than patients without aneurysm symptoms. Notably, although not statistically significant, AER_{average} (0.84 versus 0.68, $p = 0.093$) tended to be higher in patients with aneurysm symptoms. In subsequent ROC curve analyses, $CR_{\text{stalk-max}}$ had the greatest AUC of 0.697 (Figure 5). When the cut-off value of $CR_{\text{stalk-max}}$ was 0.90, the sensitivity and the specificity were 0.60 and 0.701, respectively.

Risk factors associated with AWE and $CR_{\text{stalk-max}}$ in FIAs

The cut-off value of $CR_{\text{stalk-max}}$ was 0.90. Thus, a $CR_{\text{stalk-max}}$ of ≥ 0.90 was defined as AWE, and a $CR_{\text{stalk-max}}$ of <0.90 was defined as non-AWE. For the risk factors of AWE in FIAs, univariate analysis revealed that age ($p = 0.140$), aneurysm symptoms ($p = 0.001$), hyperlipidemia ($p = 0.083$), diabetes mellitus ($p = 0.113$), coronary artery disease ($p = 0.068$), atherosclerosis ($p = 0.014$), mural thrombus ($p = 0.054$), current smoking ($p = 0.180$), aspirin use ($p = 0.044$), FIA type ($p = 0.027$), D_{max} ($p = 0.003$), L_{max} ($p = 0.003$), and posterior circulation aneurysm ($p = 0.071$) tended to be associated with positive AWE and were entered into the multivariate analysis. In the multivariate analysis, aneurysm symptoms [odds ratio (OR) = 3.754, $p = 0.003$], D_{max} (OR = 1.171, $p = 0.043$), and aspirin use (OR = 0.248, $p = 0.037$) still remained significant (Table 2).

For the risk factors of $CR_{\text{stalk-max}}$ in FIAs, univariate analysis revealed that hyperlipidemia ($p = 0.118$), current smoking ($p = 0.105$), aspirin use ($p = 0.103$), aneurysm symptoms ($p < 0.001$), posterior circulation aneurysm ($p < 0.001$), D_{max} ($p = 0.002$), L_{max} ($p < 0.001$), mural thrombus ($p = 0.004$), and atherosclerosis ($p < 0.001$) tended to be associated with $CR_{\text{stalk-max}}$ and were entered into the multivariate analysis. Multivariate analysis revealed that aneurysm symptoms (OR = 1.289, $p = 0.003$) and posterior circulation aneurysm (OR = 1.314, $p = 0.001$) were the independent predictors of $CR_{\text{stalk-max}}$ (Table 3).

Risk factors associated with FIA type

The subgroup analysis of FIA type is presented in Table 4. In the univariate analysis, transitional-type FIAs had the highest $CR_{\text{stalk-max}}$ (1.00 ± 0.25), while fusiform-type FIAs had the lowest $CR_{\text{stalk-max}}$ (0.81 ± 0.28). 93.3% of transitional-type FIAs had hypertension compared with 57.1% of dolichoectatic-type FIAs and 46.9% of fusiform-type FIAs ($p = 0.004$). Atherosclerosis was present in 66.7% of transitional-type FIAs compared with 61.9% of dolichoectatic-type FIAs and 34.6% of fusiform-type FIAs ($p = 0.018$). Mural thrombus was present in 66.7% of transitional-type FIAs compared with 33.3% of dolichoectatic-type FIAs and 30.9% of fusiform-type FIAs ($p = 0.028$). Transitional-type FIAs had the highest D_{max} (11.53 ± 3.40 mm, $p < 0.001$) and L_{max} (29.60 ± 14.63 mm, $p < 0.001$).

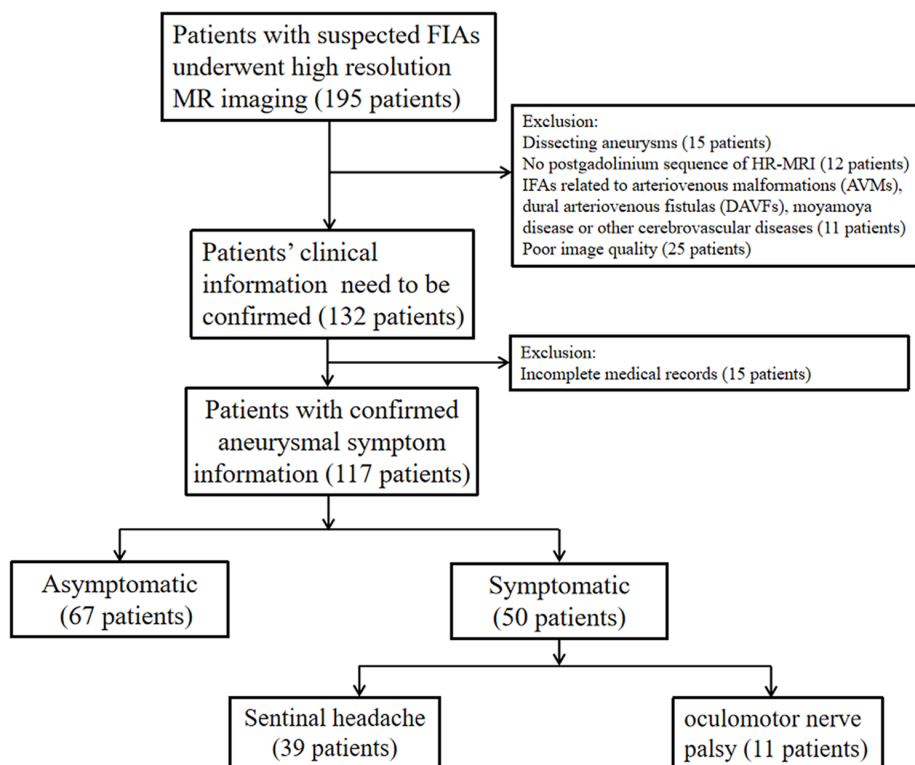


Figure 3. Flowchart of patient selection.

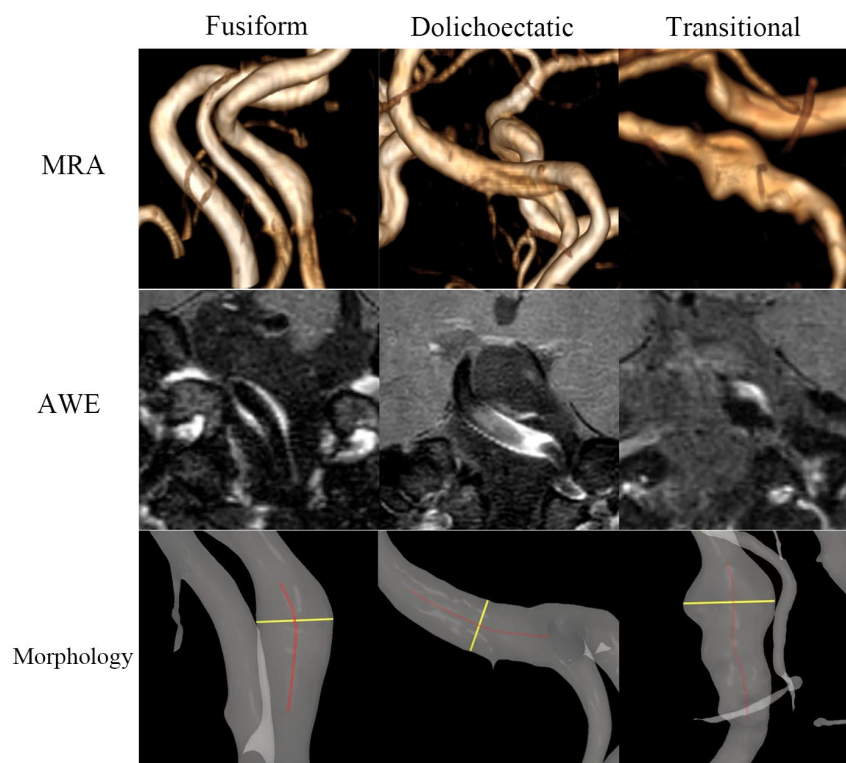


Figure 4. Assessment of aneurysm morphology and AWE in fusiform, dolichoectatic, and transitional FIAs. The upper column shows 3D TOF MRA, the middle column shows AWE of three types of FIA, and the bottom column shows D_{max} (yellow line) and L_{max} (red line).

Table 1. Characteristics of patients and FIAs.

Characteristics	
Age, mean \pm SD	53.3 \pm 11.7
Male, N (%)	88 (75.2)
Hypertension, N (%)	64 (54.7)
Hyperlipidemia, N (%)	41 (35.0)
Diabetes, N (%)	11 (9.4)
Smoking status, N (%)	
Never smoking	52 (44.4)
Current smoking	45 (38.5)
Former smoking	20 (17.1)
Location, N (%)	
Anterior circulation	18 (15.4)
Posterior circulation	99 (84.6)
CR _{stalk-max} , mean \pm SD	0.87 \pm 0.29
AER _{max} , mean \pm SD	0.98 \pm 0.64
AEI _{max} , mean \pm SD	0.94 \pm 0.61
CR _{stalk-average} , mean \pm SD	0.71 \pm 0.22
AER _{average} , mean \pm SD	0.7 \pm 0.54
AEI _{average} , mean \pm SD	0.71 \pm 0.51
Aspirin use, N (%)	19 (16.2)
D _{max} (mm)	8.83 \pm 3.15
L _{max} (mm)	18.03 \pm 10.65
AEI, aneurysm enhancement index; AER, aneurysm enhancement ratio; CR, contrast ratio; CR _{stalk} , aneurysm-to-pituitary stalk contrast ratio; SD, standard deviation.	

compared with both dolichoectatic- and fusiform-type FIAs.

In multivariate analysis, dolichoectatic-type FIAs showed higher L_{max} over fusiform-type FIA (OR=1.260, $p<0.001$). Transitional-type FIAs showed higher L_{max} (OR=1.274, $p<0.001$), higher rates of hypertension (OR=53.700, $p=0.004$), and tended to have higher rates of mural thrombus (OR=5.698, $p=0.095$) over fusiform-type FIAs. In addition, transitional-type

FIAs showed higher rates of hypertension (OR=19.411, $p=0.026$) and higher rates of mural thrombus (OR=8.146, $p=0.040$) over dolichoectatic-type FIAs.

Discussion

Poor natural history²¹ and high mortality and morbidity rates by clinical treatment (e.g. surgical clipping, bypass, or endovascular treatment)²⁵ put a dilemma for patients of whether to choose conservative treatment or aggressive intervention, especially for those patients without clear clinical symptoms. Furthermore, insufficient understanding of the intricate pathophysiology processes of FIAs may impede an effective clinical management strategy. Recently, AWE, manifested aneurysm wall pathology, has emerged as a new imaging biomarker of IA instability.²⁶ Thus, a standardized method of AWE quantification may facilitate FIA stability prediction and delineate the borderline cases that need intervention. Moreover, investigations of the influence factors of AWE and FIA types may help to understand FIA pathophysiology and contribute to clinical management.

In the present study, we found CR_{stalk-max} is the most reliable AWE quantitative parameter in distinguishing aneurysm symptoms, with a cut-off value of 0.90. Then, AWE was defined as CR_{stalk-max} \geq 0.90. We found that the independent predictors of AWE and CR_{stalk-max} may include D_{max}, aneurysm symptoms, aspirin use, and posterior circulation aneurysm. Transitional-type FIAs showed higher rates of hypertension and mural thrombus over both dolichoectatic- and fusiform-type FIAs.

Standardized AWE parameters in FIAs

Qualitative and quantitative studies of AWE have been performed in the context of SIAs.¹⁶⁻¹⁸ To identify the most reliable AWE parameters to distinguish unstable SIAs, Roa *et al.* compared three different AWE parameters (CR_{stalk}, AER, and AEI). They found that CR_{stalk} with a maximum SI had the highest sensitivity in discriminating unstable SIAs, with a cut-off value of 0.60.¹⁷ Recently, AWE of FIAs has received much attention.^{6,11,20} Liu *et al.* investigated AWE of SIAs and FIAs using 7.0-T HR-MRI. They found that compared with SIAs, FIAs had a stronger enhancement pattern, a higher enhancement grade, and a higher enhancement ratio (ER), which corresponds to

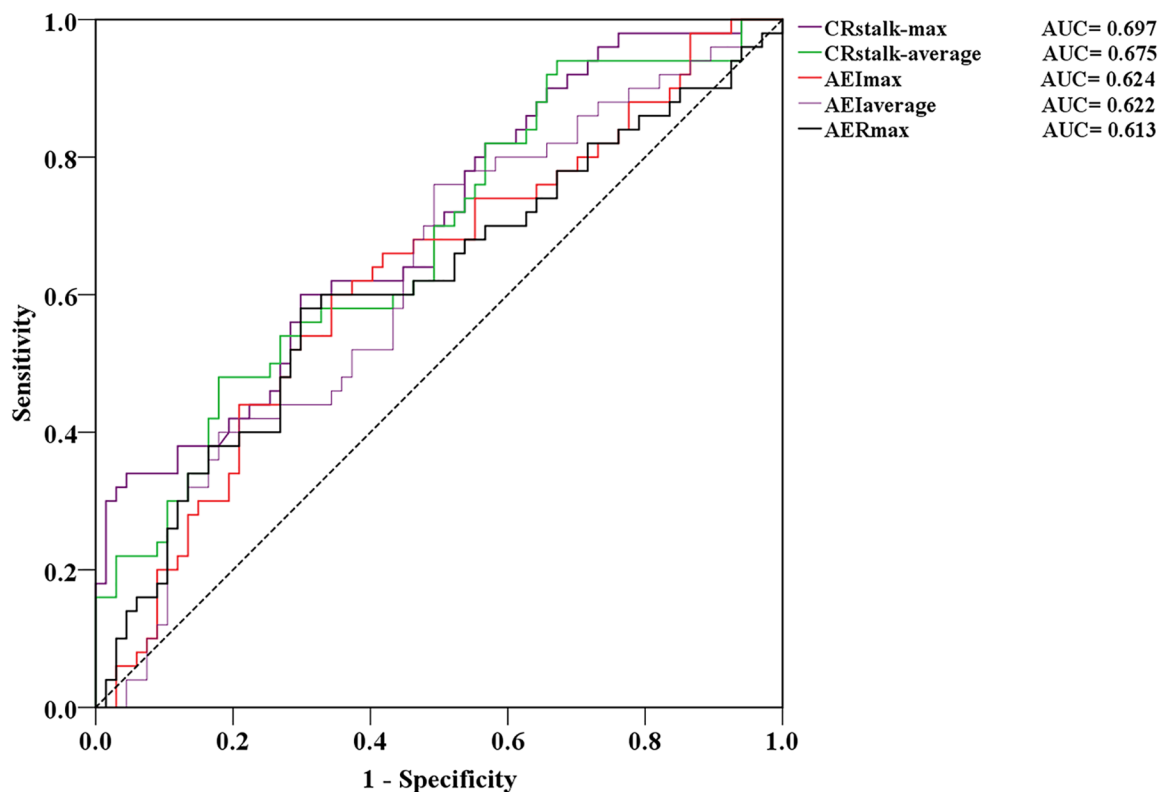


Figure 5. ROC curves for $CR_{stalk-max}$, AER_{max} , AEI_{max} , $CR_{stalk-average}$, and $AEI_{average}$ with AUC values of 0.697, 0.675, 0.624, 0.622, and 0.613, respectively.

CR_{stalk} in the current study.⁶ In their study, the average maximum ER and mean ER values in FIAs were 1.42 and 0.96, respectively. Cao *et al.*²⁰ investigated the AWE characteristics of non-saccular aneurysms in the basilar and vertebral arteries. They found that ER was an independent predictor of aneurysm symptoms, with a cut-off value of 0.82. However, related studies on AWE quantification in FIAs are still limited. Furthermore, the cut-off value for AWE, which can differentiate unstable FIAs, is still unclear. Roa *et al.*¹⁷ defined those unruptured SIAs ≥ 7 mm in certain locations (e.g. anterior communicating, posterior communicating, and basilar arteries) as unstable. In the current study, unstable FIAs were defined as certain symptoms (sentinel headache and oculomotor nerve palsy), since they are reportedly strongly indicative of aneurysm instability.¹⁶ Therefore, we compared CR_{stalk} , AER, and AEI with the maximum and mean SI in their ability to distinguish aneurysm symptoms. We found that CR_{stalk} with a maximum SI ($CR_{stalk-max}$) had the highest accuracy in identifying symptomatic FIAs, with a cut-off value of 0.90. Thus, $CR_{stalk-max}$ (≥ 0.90) may also have the potential to

distinguish unstable FIAs. For example, an FIA with $CR_{stalk-max} \geq 0.90$ (especially for those patients with unspecific symptoms) may indicate unstable and require clinical evaluation or further intervention. In addition, the pathophysiology of IAs includes the interaction between morphology, hemodynamics, and aneurysm inflammation.^{10,27} Hence, in future studies, we consider AWE could be combined with the current risk factors of IA instability (e.g. symptom, aneurysm size) to establish a comprehensive evaluation model for IA stability.

Risk factors for AWE and $CR_{stalk-max}$ of FIAs

On the basis of the cut-off value of 0.90, parameter of AWE was divided into AWE and non-AWE. D_{max} , aspirin use, and aneurysm symptoms were independent predictors of AWE in FIAs. A previous study demonstrated the association between AWE and D_{max} .²⁰ Moreover, AWE correlated with aneurysm growth in several previous studies and tended to be greater when close to the SIA neck.^{28–30} D_{max} represents the most obvious expansion of the cross-sectional plane; thus, this

Table 2. Uni- and multivariate analyses using $CR_{\text{stalk-max}} \geq 0.90$ as the cut-off for aneurysmal wall enhancement.

Variables	Univariate		Multivariate	
	OR (95% CI)	<i>p</i> value	OR (95% CI)	<i>p</i> value
Age	–	0.140	0.998 (0.957–1.040)	0.910
Male	0.929 (0.397–2.175)	1.000	–	–
Aneurysm symptoms	3.525 (1.631–7.618)	0.001	3.754 (0.129–0.680)	0.003*
Hypertension	0.952 (0.456–1.986)	1.000	–	–
Hyperlipidemia	0.489 (0.221–1.086)	0.083	0.510 (0.202–1.284)	0.153
Diabetes	0.269 (0.055–1.303)	0.113	0.428 (0.068–2.708)	0.367
Coronary artery disease	0.238 (0.050–1.137)	0.068	0.576 (0.076–4.354)	0.593
Stroke history	0.830 (0.349–1.973)	0.827	–	–
Atherosclerosis	2.642 (1.242–5.620)	0.014	1.770 (0.637–4.922)	0.274
Mural thrombus	2.152 (0.997–4.644)	0.054	2.284 (0.922–5.657)	0.074
Current smoking	1.742 (0.819–3.705)	0.180	1.4472 (0.568–3.685)	0.438
Aspirin use	0.301 (0.093–0.973)	0.044	0.248 (0.067–0.919)	0.037*
FIA types	–	0.027	1.306 (0.654–2.610)	0.450
D_{max}	–	0.003	1.171 (1.005–1.365)	0.043*
L_{max}	–	0.003	1.009 (0.949–1.073)	0.771
Posterior circulation	3.038 (0.934–9.879)	0.071	3.050 (0.847–10.982)	0.088

CI, confidence interval; CR_{stalk} , aneurysm-to-pituitary stalk contrast ratio; OR, odds ratio.
*Statistically significant.

plane tends to have stronger AWE. Therefore, it is more inclined to grow. L_{max} , based on the 3D vessel model and centerline extraction, was used to define the length of the culprit vessel. L_{max} was not an independent predictor of AWE in this study, possibly due to the heterogeneity in AWE in different areas of the involved aneurysm segment.²⁸ Although D_{max} and L_{max} tended to be positively associated with $CR_{\text{stalk-max}}$ ($r_s = 0.507$, $p < 0.001$; $r_s = 0.295$, $p = 0.001$, respectively), both of them were not the independent predictors of $CR_{\text{stalk-max}}$. Thus, the associations between aneurysm morphology and AWE in FIAs need to be further verified. Aneurysm symptoms were independent predictors of both AWE and $CR_{\text{stalk-max}}$ in FIAs. Such associations between them have been reported previously.^{16,20} Anti-inflammatory drugs, such as aspirin, are associated with a decrease in AWE in SIAs.¹⁷ In the

current study, aspirin use was the independent predictor of AWE in FIAs. Aspirin is beneficial in resisting the inflammatory microenvironment in the aneurysm wall through its ability to inhibit COX-2 activity, which is involved in aneurysm pathogenesis and progression.^{17,31} Considering aspirin use has been reported to be associated with a decreased risk of aneurysm growth in SIAs,^{32,33} it may also have the potential to decrease the growth rate of FIAs. However, aspirin use was not the independent predictor of $CR_{\text{stalk-max}}$. In fact, only 19 patients (16.2%) had a history of aspirin use in the recent 6 months or longer, which may limit the results compared with a recent study in which a high proportion of patients (52.7%) used aspirin.¹⁷ Other risk factors (e.g. mural thrombus, posterior circulation, atherosclerosis) also tended to be associated with AWE (or $CR_{\text{stalk-max}}$) in FIAs although did not reach

Table 3. Risk factors associated with CR_{stalk} .

Variables	Univariate analysis		Multivariate analysis ($R^2 = 0.374, p < 0.001$)	
	Beta	p value	Beta	p value
Demographic data				
Age, years	-0.006	0.952	-	-
Male patients, N (%)	0.029	0.754	-	-
Risk factors				
Hypertension	0.029	0.755	-	-
Diabetes	-0.178	0.055	-0.091	0.265
Hyperlipidemia	-0.145	0.118	-0.122	0.137
Current smoker	0.151	0.105	0.052	0.526
Aspirin use	-0.151	0.103	-0.154	0.062
Cardiovascular disease	-0.084	0.366	-	-
History of stroke	-0.058	0.535	-	-
Aneurysm symptoms				
Posterior circulation	0.325	<0.001*	0.273	0.001*
D_{max} , mm	0.280	0.002*	0.031	0.750
L_{max} , mm	0.319	<0.001*	0.123	0.206
Mural thrombus, N (%)	0.266	0.004*	0.142	0.128
Atherosclerosis	0.353	<0.001*	0.184	0.063

CR, contrast ratio CR_{stalk} , aneurysm-to-pituitary stalk contrast ratio.
* $p < 0.05$.

statistical significance, larger cohorts are needed to investigate and validate such risk factors.

Risk factors for FIA types

Compared with SIAs, FIAs have a different pathogenesis and tend to involve the entire artery.¹¹ Flemming *et al.*⁹ made a simple classification for FIA types (fusiform, dolichoectatic, and transitional) based on the extent of dilatation and the involved artery. Because of limited studies on FIAs, the potential risk factors that differentiate the types of FIA are still unclear. Nasr *et al.* performed a subgroup analysis of FIA types. They found significant differences in maximum diameter and mural thrombus between the three FIA types.²¹ Compared with their study, HR-MRI was

used in the present study to present the characteristics of aneurysm wall vasculopathy and aneurysm morphology, which revealed that transitional-type FIAs had higher rates of hypertension and mural thrombus than both dolichoectatic- and fusiform-type FIAs (Table 4). Hypertension has long been considered an independent predictor of IAs.³⁴ This all revealed that hypertension may facilitate the evolution of FIAs to a more complex type (transitional-type). Mural thrombus also occurred more often in transitional-type FIAs than in the other two FIA types. Mural thrombus, which manifests the processes of neovascularization in the inner aneurysmal wall or vasa vasorum in the outer aneurysmal wall,^{8,35} was reported to be a predictor of FIA growth.²¹ Therefore, FIA patients with hypertension need more close blood pressure monitoring.³⁶ In addition, on the basis of the 3D vessel model, L_{max} tended to be longer in dolichoectatic- and transitional-type FIAs than in fusiform-type FIAs (Table 4), which revealed that more complex types of FIAs tend to involve more areas of the culprit artery. Still, longitudinal follow-up studies based on HR-MRI with larger sample sizes are needed to investigate the differences in progression between the three types of FIA.

The findings of this study have several clinical implications. First, $CR_{\text{stalk-max}}$ could serve as a new imaging biomarker of FIA symptoms (sentinel headache and oculomotor nerve palsy) for patient screening. Second, an FIA with $CR_{\text{stalk-max}}$ of ≥ 0.90 may indicate the FIA is unstable, especially for patients with unclear clinical symptoms and hard to assess the FIA stability. Third, FIA patients with hypertension need close monitoring and management of hypertension. Finally, anti-inflammatory drugs (e.g. aspirin) may have the potential to decrease AWE and therefore inhibit FIA progression further.

Strengths and limitations

To our knowledge, this is the first study to quantitatively evaluate the ability of AWE to discriminate aneurysm symptoms in a large cohort of patients with FIAs based on HR-MRI. In addition, the risk factors for AWE and FIA types were also investigated. To eliminate the heterogeneity between the three types of FIA to the greatest possible extent, dissecting aneurysms were excluded from the current study, which was in accordance with a previous study.²¹ However, the

Table 4. Uni- and multivariate analyses for FIA types.

Other risk factors	Univariate analysis			Multivariate analysis					
	Fusiform (N=81)	Dolichoectatic (N=21)	Transitional (N=15)	Translational versus fusiform		Dolichoectatic versus fusiform		Translational versus dolichoectatic	
				OR (95% CI)	p value	OR (95% CI)	p value	OR (95% CI)	p value
Mean age (SD)	53.16 ± 12.54	53.19 ± 10.79	54.4 ± 8.57	-	0.945	-	-	-	-
Male, N (%)	60 (74.1)	15 (71.4)	13 (86.7)	-	0.529	-	-	-	-
CR _{statik-max} , mean ± SD	0.81 ± 0.28	0.99 ± 0.29	1.00 ± 0.25	1.057 (0.038–29.087)	0.974	3.478 (0.316–38.240)	0.308	0.304 (0.012–8.025)	0.476
Aspirin use, N (%)	11 (13.6%)	5 (23.8%)	3 (20.0%)	-	0.481	-	-	-	-
Hypertlipidemia, N (%)	30 (37.0%)	6 (28.6%)	5 (33.3%)	-	0.761	-	-	-	-
Hypertension, N (%)	38 (46.9%)	12 (57.1%)	14 (93.3%)	53.7 (3.602–800.536)	0.004*	2.766 (0.701–10.919)	0.146	19.411 (1.424–264.659)	0.026*
Diabetes, N (%)	7 (8.6%)	4 (19.0%)	0 (0%)	-	0.142	-	-	-	-
Coronary artery disease, N (%)	7 (8.6%)	4 (19.0%)	1 (6.7%)	-	0.332	-	-	-	-
Stroke history, N (%)	18 (22.2%)	6 (28.6%)	4 (26.7%)	-	0.332	-	-	-	-
Atherosclerosis, N (%)	28 (34.6%)	13 (61.9%)	10 (66.7%)	0.208 (0.023–1.916)	0.018*	0.720 (0.160–3.243)	0.669	0.289 (0.030–2.760)	0.281
Current smoking, N (%)	29 (35.8%)	8 (38.1%)	8 (53.3%)	-	0.439	-	-	-	-
Mural thrombus	25 (30.9)	7 (33.3)	10 (66.7)	5.698 (0.738–43.967)	0.028*	0.700 (0.161–3.032)	0.633	8.146 (1.100–60.297)	0.040*
D _{max} , mean ± SD	7.98 ± 2.59	10.00 ± 3.7	11.53 ± 3.40	<0.001*	1.240 (0.919–1.673)	0.159	1.015 (0.804–1.281)	1.222 (0.934–1.599)	0.144
L _{max} , mean ± SD	13.44 ± 5.52	27.62 ± 10.19	29.60 ± 14.63	<0.001*	1.274 (1.131–1.435)	<0.001*	1.260 (1.136–1.398)	1.012 (0.937–1.092)	0.768
Posterior circulation, N (%)	68 (84.0%)	16 (76.2%)	15 (100%)	-	0.142	-	-	-	-

CI, confidence interval; OR, odds ratio; SD, standard deviation.
*Statistically significant.

present study had several limitations. First, this is a retrospective study. Second, HR-MRI images were exported from three different 3.0-T MRI machines, although the inherent parameters were adjusted to ensure consistency. In addition, the voxel size is 0.7 mm, which is oversized for most of the aneurysmal walls. Third, this study is lacking in histologic verification. Fourth, further follow-up studies with larger sample sizes are needed to make more intergroup comparisons. In the future, considering the relatively low sensitivity and specificity of predicting AWE in the current study, more accurate methods, such as 3D space technology, are needed to quantify AWE.

Conclusion

$CR_{\text{stalk-max}}$ may be the most reliable parameter of AWE quantification to distinguish symptomatic FIAs, thus, it also has the potential to distinguish unstable FIAs. Predictors of AWE in FIAs may include D_{max} , aneurysm symptoms, aspirin use, and posterior circulation aneurysm. Transitional-type FIAs showed higher rates of hypertension and mural thrombus over both dolichoectatic- and fusiform-type FIAs. Moreover, longitudinal follow-up studies based on HR-MRI with larger sample sizes are needed to further understand the physiological mechanisms of FIAs.

Declarations

Ethics approval and consent to participate

This study was approved by the institutional ethics committee of Beijing Tiantan Hospital (KY 2018-086-03). Written informed consent was provided by each subject.

Consent for publication

Not applicable.

Author contributions

Fei Peng: Investigation; Methodology; Writing – original draft.

Mingzhu Fu: Investigation; Methodology; Writing – original draft.

Jiaxiang Xia: Investigation; Methodology; Writing – original draft.

Hao Niu: Conceptualization; Data curation; Resources.

Lang Liu: Conceptualization; Data curation; Resources.

Xin Feng: Conceptualization; Data curation; Resources.

Peng Xu: Conceptualization; Data curation; Resources.

Xiaoyan Bai: Conceptualization; Data curation; Resources.

Zhiye Li: Conceptualization; Data curation; Resources.

Jigang Chen: Conceptualization; Data curation; Resources.

Xin Tong: Conceptualization; Data curation; Resources.

Xiaoxin He: Formal analysis; Resources; Software; Validation.

Boya Xu: Formal analysis; Resources; Software; Validation.

Xuge Chen: Data curation; Resources; Software; Validation.

Hongyi Liu: Formal analysis; Resources; Software; Validation.


Binbin Sui: Supervision; Validation; Writing – review & editing.

Yonghong Duan: Supervision; Validation; Writing – review & editing.

Rui Li: Project administration; Supervision; Writing – review & editing.

Aihua Liu: Project administration; Supervision; Writing – review & editing.

ORCID iD

Aihua Liu  <https://orcid.org/0000-0002-6391-805X>

Funding

The authors disclosed receipt of the following financial support for the research, authorship, and/or publication of this article: This work was supported by the Natural Science Foundation of China (grant nos. 81771233 and 82171290), Natural Science Foundation of Beijing, China (grant nos. 7142032 and L192013), Specific Research Projects for Capital Health Development (grant no. 2018-2-2041), Beijing Science and Technology Planning Project (grant no. Z181100009618035), Beijing Municipal Administration of Hospitals' Ascent Plan (grant no. DFL20190501), Horizontal Project in

Beijing Tiantan Hospital [grant no. HX-A-043 (2021)], Research and Promotion Program of Appropriate Techniques for Intervention of Chinese High-risk Stroke People (grant no. GN-2020R0007).

Competing Interests

The authors declared no potential conflicts of interest with respect to the research, authorship, and/or publication of this article.

Availability of data and materials

Not applicable.

References

- Vlak MH, Algra A, Brandenburg R, *et al.* Prevalence of unruptured intracranial aneurysms, with emphasis on sex, age, comorbidity, country, and time period: a systematic review and meta-analysis. *Lancet Neurol* 2011; 10: 626–636.
- Biondi A. Trunkal intracranial aneurysms: dissecting and fusiform aneurysms. *Neuroimaging Clin N Am* 2006; 16: 453–465, viii.
- Liu X, Zhang Z, Zhu C, *et al.* Wall enhancement of intracranial saccular and fusiform aneurysms may differ in intensity and extension: a pilot study using 7-T high-resolution black-blood MRI. *Eur Radiol* 2020; 30: 301–307.
- Anson JA, Lawton MT and Spetzler RF. Characteristics and surgical treatment of dolichoectatic and fusiform aneurysms. *J Neurosurg* 1996; 84: 185–193.
- Wagner A, Prothmann S, Hedderich D, *et al.* Fusiform aneurysms of the vertebrobasilar complex: a single-center series. *Acta Neurochir* 2020; 162: 1343–1351.
- Park SH, Yim MB, Lee CY, *et al.* Intracranial fusiform aneurysms: it's pathogenesis, clinical characteristics and managements. *J Korean Neurosurg Soc* 2008; 44: 116–123.
- Castle-Kirsbaum M, Maingard J, Lim RP, *et al.* Four-dimensional magnetic resonance imaging assessment of intracranial aneurysms: a state-of-the-art review. *Neurosurgery* 2020; 87: 453–465.
- Sabotin RP, Varon A, Roa JA, *et al.* Insights into the pathogenesis of cerebral fusiform aneurysms: high-resolution MRI and computational analysis. *J Neurointerv Surg* 2021; 13: 1180–1186.
- Flemming KD, Wiebers DO, Brown RD Jr, *et al.* The natural history of radiographically defined vertebrobasilar nonsaccular intracranial aneurysms. *Cerebrovasc Dis* 2005; 20: 270–279.
- Turjman AS, Turjman F and Edelman ER. Role of fluid dynamics and inflammation in intracranial aneurysm formation. *Circulation* 2014; 129: 373–382.
- Shimonaga K, Matsushige T, Ishii D, *et al.* Clinicopathological insights from vessel wall imaging of unruptured intracranial aneurysms. *Stroke* 2018; 49: 2516–2519.
- Larsen N, von der Brölie C, Trick D, *et al.* Vessel wall enhancement in unruptured intracranial aneurysms: an indicator for higher risk of rupture? High-resolution MR imaging and correlated histologic findings. *Am J Neuroradiol* 2018; 39: 1617–1621.
- Roa JA, Zanaty M, Osorno-Cruz C, *et al.* Objective quantification of contrast enhancement of unruptured intracranial aneurysms: a high-resolution vessel wall imaging validation study. *J Neurosurg* 2020; 134: 862–869.
- Edjlali M, Gentric JC, Régent-Rodriguez C, *et al.* Does aneurysmal wall enhancement on vessel wall MRI help to distinguish stable from unstable intracranial aneurysms? *Stroke* 2014; 45: 3704–3706.
- Omodaka S, Endo H, Niizuma K, *et al.* Quantitative assessment of circumferential enhancement along the wall of cerebral aneurysms using MR imaging. *Am J Neuroradiol* 2016; 37: 1262–1266.
- Fu Q, Wang Y, Zhang Y, *et al.* Qualitative and quantitative wall enhancement on magnetic resonance imaging is associated with symptoms of unruptured intracranial aneurysms. *Stroke* 2021; 52: 213–222.
- Roa JA, Zanaty M, Ishii D, *et al.* Decreased contrast enhancement on high-resolution vessel wall imaging of unruptured intracranial aneurysms in patients taking aspirin. *J Neurosurg* 2020; 134: 902–908.
- Swiatek VM, Neyazi B, Roa JA, *et al.* Aneurysm wall enhancement is associated with decreased intrasaccular IL-10 and morphological features of instability. *Neurosurgery* 2021; 89: 664–671.
- Feng X, Qian Z, Zhang B, *et al.* Number of cigarettes smoked per day, smoking index, and intracranial aneurysm rupture: a case-control study. *Front Neurol* 2018; 9: 380.
- Cao L, Zhu C, Eisenmenger L, *et al.* Wall enhancement characteristics of vertebrobasilar nonsaccular aneurysms and their relationship to symptoms. *Eur J Radiol* 2020; 129: 109064.

21. Nasr DM, Brinjikji W, Rouchaud A, *et al.* Imaging characteristics of growing and ruptured vertebralbasilar non-saccular and dolichoectatic aneurysms. *Stroke* 2016; 47: 106–112.
22. Jung SC, Kim HS, Choi CG, *et al.* Spontaneous and unruptured chronic intracranial artery dissection: high-resolution magnetic resonance imaging findings. *Clin Neuroradiol* 2018; 28: 171–181.
23. Day AL, Gaposchkin CG, Yu CJ, *et al.* Spontaneous fusiform middle cerebral artery aneurysms: characteristics and a proposed mechanism of formation. *J Neurosurg* 2003; 99: 228–240.
24. Moon J, Cho YD, Yoo DH, *et al.* Growth of asymptomatic intracranial fusiform aneurysms: incidence and risk factors. *Clin Neuroradiol* 2019; 29: 717–723.
25. Turhon M, Kang H, Li M, *et al.* Treatment of fusiform aneurysms with a pipeline embolization device: a multicenter cohort study. *J Neurointerv Surg*. Epub ahead of print 30 March 2022. DOI: 10.1136/neurintsurg-2021-018539.
26. Wang GX, Wen L, Lei S, *et al.* Wall enhancement ratio and partial wall enhancement on MRI associated with the rupture of intracranial aneurysms. *J Neurointerv Surg* 2017; 10: 566–570.
27. Lv N, Karmonik C, Chen S, *et al.* Wall enhancement, hemodynamics, and morphology in unruptured intracranial aneurysms with high rupture risk. *Transl Stroke Res* 2020; 11: 882–889.
28. Samaniego EA, Roa JA, Zhang H, *et al.* Increased contrast enhancement of the parent vessel of unruptured intracranial aneurysms in 7T MR imaging. *J Neurointerv Surg* 2020; 12: 1018–1022.
29. Gariel F, Ben Hassen W, Boulouis G, *et al.* Increased wall enhancement during follow-up as a predictor of subsequent aneurysmal growth. *Stroke* 2020; 51: 1868–1872.
30. Hashimoto Y, Matsushige T, Kawano R, *et al.* Segmentation of aneurysm wall enhancement in evolving unruptured intracranial aneurysms. *J Neurosurg* 2021; 136: 449–445.
31. Hasan D, Hashimoto T, Kung D, *et al.* Upregulation of cyclooxygenase-2 (COX-2) and microsomal prostaglandin E2 synthase-1 (mPGES-1) in wall of ruptured human cerebral aneurysms: preliminary results. *Stroke* 2012; 43: 1964–1967.
32. Zanaty M, Roa JA, Nakagawa D, *et al.* Aspirin associated with decreased rate of intracranial aneurysm growth. *J Neurosurg*. Epub ahead of print 29 October 2019. DOI: 10.3171/2019.6.JNS191273.
33. Weng JC, Wang J, Li H, *et al.* Aspirin and growth of small unruptured intracranial aneurysm: results of a prospective cohort study. *Stroke* 2020; 51: 3045–3054.
34. Tada Y, Wada K, Shimada K, *et al.* Roles of hypertension in the rupture of intracranial aneurysms. *Stroke* 2014; 45: 579–586.
35. Sato T, Matsushige T, Chen B, *et al.* Wall contrast enhancement of thrombosed intracranial aneurysms at 7T MRI. *Am J Neuroradiol* 2019; 40: 1106–1111.
36. Zhong P, Lu Z, Li T, *et al.* Association between regular blood pressure monitoring and the risk of intracranial aneurysm rupture: a multicenter retrospective study with propensity score matching. *Transl Stroke Res*. Epub ahead of print 21 March 2022. DOI: 10.1007/s12975-022-01006-7.